1983

The construction of a Nd: YAG laser and observation of the output

Chung, Ki Hyun

Monterey, California. Naval Postgraduate School

NAVAL POSTGRADUATE SCHOOL
Monterey, California

THESIS

THE CONSTRUCTION OF A Nd:YAG LASER
AND OBSERVATION OF THE OUTPUT

by

Ki Hyun Chung

December 1983

Thesis Advisor: A. W. Cooper

REPORT DOCUMENTATION PAGE

READ INSTRUCTIONS BEFORE COMPLETING FORM

1. REPORT NUMBER

2. GOVT ACCESSION NO.

3. RECIPIENT'S CATALOG NUMBER

4. TITLE (and Subtitle)

The Construction of a Nd:YAG Laser and Observation of the Output

5. TYPE OF REPORT & PERIOD COVERED
Master's Thesis
December 1983

6. PERFORMING ORG. REPORT NUMBER

7. AUTHOR(s)

Ki Hyun Chung

8. CONTRACT OR GRANT NUMBER(s)

9. PERFORMING ORGANIZATION NAME AND ADDRESS
Naval Postgraduate School
Monterey, California 93943

10. PROGRAM ELEMENT, PROJECT, TASK AREA & WORK UNIT NUMBERS

11. CONTROLLING OFFICE NAME AND ADDRESS
Naval Postgraduate School
Monterey, California 93943

12. REPORT DATE
December 1983

13. NUMBER OF PAGES
63

14. MONITORING AGENCY NAME & ADDRESS(if different from Controlling Office)

15. SECURITY CLASS. (of this report)
Unclassified

15a. DECLASSIFICATION/DOWNGRADING SCHEDULE

16. DISTRIBUTION STATEMENT (of this Report)

Approved for public release; distribution unlimited.

17. DISTRIBUTION STATEMENT (of the abstract entered in Block 20, if different from Report)

18. SUPPLEMENTARY NOTES

19. KEY WORDS (Continue on reverse side if necessary and identify by block number)
Laser, Nd:YAG

20. ABSTRACT (Continue on reverse side if necessary and identify by block number)
An experimental Neodymium YAG laser system has been constructed using a cylindrical pumping reflector containing three CW tungsten-halide lamps. Maximum laser output of 2.05 watts has been obtained with slope efficiency 0.19 percent at 3300 watts input power. Slope efficiency increased with increasing input power, and output power decreased with increasing resonator length.

Approved for public release; distribution unlimited.

The Construction of a Nd:YAG Laser and Observation of the Output

by

Ki Hyun Chung
Major, Republic of Korea Army
B.S., Korean Military Academy, 1976

Submitted in partial fulfillment of the
requirements for the degree of

MASTER OF SCIENCE IN PHYSICS

from the

NAVAL POSTGRADUATE SCHOOL
December 1983

ABSTRACT

An experimental CW Neodymium-YAG laser has been constructed using a gold coated circular cylindrical pumping cavity. The rod is located along the cylinder axis and is pumped by three tungsten-halide filament lamps symmetrically spaced at equal radial distances from the rod. The resonator consists of a concave 100 percent reflecting mirror and a flat output mirror with variable axial spacing.

Lasing threshold was achieved at an input power of 2000 watts with the lamps 12 millimeters from the rod, using a 6.1 percent transmittance output mirror. Threshold was not achieved with a 27 percent transmittance mirror.

A maximum CW output of 2.05 watts was observed with 3300 watts input power. The maximum slope efficiency at the maximum available power of 3300 watts was measured as 0.19 percent, which is considerably lower than found in commercial systems using elliptical cavities. The slope efficiency increased with increase in the input power; this was probably due to the change in the wavelength of the peak emission from the lamps. The optimized output power was greatest at the minimum resonator length of approximately one half the mirror radius of curvature, and reached a minimum at one radius of curvature spacing.

TABLE OF CONTENTS

I. INTRODUCTION 8

II. THEORETICAL 10

A. PROPERTIES OF Nd:YAG CRYSTAL 11

1. Physical Properties 11

2. Laser Properties 12

B. OPTICAL RESONATOR 18

1. Resonator Configuration 18

2. Stability of Laser Resonator 21

3. Loss in Optical Resonator 22

C. OPTICAL PUMPING SYSTEM 24

1. Pumping Sources 24

2. Pumping Cavities 27

3. Efficiencies 30

D. HEAT REMOVAL 31

1. Thermal Effects in the Laser Rod 32

2. Cooling Techniques 34

III. EXPERIMENTAL INVESTIGATION 37

A. CONSTRUCTION OF THE SYSTEM 37

1. Optical Resonator 37

2. Optical Pumping System 38

3. Cooling System 39

4. Assembly of the System 40

B. OPERATION OF THE LASER 42

1. Measurement of Fluorescence 42

2. Measurement of Laser Output 43

C. DISCUSSION 48

IV. CONCLUSIONS 53

APPENDIX A DETAILS OF PUMPING-CAVITY HEAD 55

LIST OF REFERENCES 61

INITIAL DISTRIBUTION LIST 63

LIST OF TABLES

1. Properties of Nd:YAG 15

2. Absorption Spectrum of Nd in YAG [Ref. 6] 17

3. Properties of Mirrors for Experimental Laser Systems 37

4. Laser Action with Different Combinations of Mirrors 44

LIST OF FIGURES

1. Energy Level Diagram of Nd:YAG 14

2. Fluorescence Spectrum of Nd^{3+} in YAG at 300°K in the Region of 1.06μm 14

3. Absorption Spectrum of Nd:YAG 16

4. Energy Level of Nd:YAG Related to Absorption Spectrum 16

5. Diffraction Loss for a Plane-Parallel and Several Low-Order Confocal Resonators 23

6. Spectral Emission of Xenon Flash Tube 26

7. Emission Spectrum of a CW-pumped Krypton Arc Lamp (6mm bore, 50 mm Arc Length, 1.3 kw Input) . . . 26

8. Relative Performance of Krypton, Xenon and Tungsten-Iodine Lamps for Continuous Pumping of Nd:YAG . . . 27

9. Characteristic Configurations of Pumping Cavity . . 29

10. Basic Assembly of Experimental System 41

11. Detector System Alignment 41

12. Measurement of Fluorescence Power 45

13. Laser Output of Experimental System 46

14. Maximum Output with Change of the Spacing of the Resonator Mirrors 47

I. INTRODUCTION

Nd:YAG is one of the most widely used laser materials, with a lasing wavelength 1.06μm in the near infrared region. The cubic structure of YAG favors a narrow fluorescent line width which results in high gain and low threshold for laser operation. This wavelength is located beyond the visible region and the system can be operated with low input power. With these advantages, many military devices have been developed.

A Nd:YAG laser system was constructed by Jung [Ref. 1] in 1982 with a cylindrical cavity, and 0.3 watts of output was observed with 4400 watts of input, at 0.04 percent slope efficiency.

The intent of this experiment was to improve the efficiency of this system and to observe the output variations related to imput power and resonator characteristics.

The laser output was measured with different combinations of resonator mirrors and different spacings of the resonator mirrors in the stable range of resonator configuration.

In this thesis a cylindrical pumping cavity was used since the available machine shop facilities were unable to construct the original elliptical cross-section design

within the time frame of the study. The circular cylindrical cavity has lower transfer efficiency.

The rod and cavity wall were cooled by flowing coolant, and heated air was blown out with an electric fan.

II. THEORETICAL

More than two decades have passed since the discovery of laser action in ruby. Many kinds of laser active materials, which have the properties of sharp fluorescence lines, strong absorption bands and high quantum efficiencies for the fluorescence transition, have been discovered during the last two decades. Nd^{3+} was the first of the trivalent ions to be used in a laser, and it remains by far the most important element. Stimulated emission has been obtained with this ion incorporated in at least 40 different host materials. Yttrium Aluminum Garnet (YAG) is a host material with the attractive properties of hardness, chemical inertness, low internal strain and small refractive index variation.

To achieve high efficiency, well designed pumping cavities and pumping sources are required. Elliptical cylinders are most widely used in laser systems with linear pumping sources, with the lamp and rod located on the focal lines of the elliptical cylindrical reflector. The types of pumping cavities and sources are correlated to each other to concentrate the power on the laser active materials.

Optical resonators are used primarily in order to build up large field intensities with moderate power input. The

commonly used laser resonators are composed of two spherical or flat mirrors facing each other.

A. PROPERTIES OF Nd:YAG CRYSTAL

In Nd:YAG about one percent of Yttrium is substituted by Neodymium. The host material ($Y_2Al_5O_{12}$) is a colorless, optically isotropic crystal which possesses the cubic structure characteristic of garnets. With the addition of large amounts of neodymium, strained crystals are obtained since the radii of Y^{3+} and Nd^{3+} differ by about three percent. The laser transition, having a wavelength of 10641A, originates from the R_2 component of the $^4F_{3/2}$ level and terminates at the Y_3 component of the $^4I_{11/2}$ level.

1. Physical Properties

The garnets crystallize with the general formula ($A_2B_5O_{12}$) with eight such molecules contained with the unit cell. The A type (Y^{3+}) ions occupy 24 dodecahedral sites with eightfold oxygen coordination and there are 40 B type (Al^{3+}) ions divided among 24 tetrahedral d-sites with fourfold oxygen coordination and 16 octahedral sites with sixfold oxygen coordination. There are then 160 atoms within the unit cell with cube edge 12.01 ± 0.02Å in case of YAG. The YAG structure is stable from the lowest temperatures up to the melting point, and composed of 37.5 percent Y_2O_3 and 62.5 percent Al_2O_3 ($3Y_2O_3 \cdot 5Al_2O_3$).

The refractive index of YAG decreases slightly as the wavelength increases, from 1.820 at 1μm wavelength to 1.803 at 2μm wavelength. The price of Nd:YAG is relatively high since the crystal growth rate is low, 5mm per hour by the Czochralski growth method. Typical boules of 10 to 15 cm in length require a growth run of several weeks.

Neodymium concentration by atoms in YAG has been limited to 1.0 to 1.5 percent. Higher doping levels tend to shorten the fluorescent lifetime, broaden the line width and cause strain in the crystal, resulting in poor optical quality. Some of the physical properties of YAG are given in Table 1.

2. Laser Properties

The neodymium ion contains three electrons in the 4f shell with ground state configuration $^4I_{9/2}$. Three groups of transitions have been observed in the infrared absorption spectrum between 2000 and 6800 cm^{-1}. Table 2 represents the absorption spectrum of Nd^{3+} in YAG [Ref. 2].

The Nd:YAG laser is a four level system, with the energy levels shown in Figure 1 [Ref. 3]. The laser transition originates from the R_2 component of the $^4F_{3/2}$ level and terminates at the Y_3 component of the $^4I_{11/2}$ level at room temperature. At low temperature, about 77K, it was observed that the laser transition was from the R_1 component of the $^4F_{3/2}$ to the Y_1 component of the

$^4I_{11/2}$ state with wavelength 1.061μm. There are a number of levels, which together may be viewed as comprising the pump level.

The upper laser level, $^4F_{3/2}$, has fluorescent efficiency greater than 99.5 percent and radiative lifetime of 230μs. The branching ratio of emission from $^4F_{3/2}$ is as follows; $^4F_{3/2} \rightarrow {}^4I_{9/2} = 0.25$, $^4F_{3/2} \rightarrow {}^4I_{11/2} = 0.60$, $^4F_{3/2} \rightarrow {}^4I_{13/2} = 0.14$ and $^4F_{3/2} \rightarrow {}^4I_{15/2} < 0.01$ [Ref. 4]. This means almost all the ions transferred from the ground level to the pump bands end up at the upper laser level, and 60 percent of the ions at the upper laser level cause fluorescent output at the $^4I_{11/2}$ manifold. The relaxation time ($^4I_{11/2} \rightarrow {}^4I_{9/2}$) is fast enough, 30 ns, to allow the crystal to support continuous wave lasing action at room temperature.

Figure 2 shows the fluorescence spectrum of Nd^{3+} in YAG near the region of the various transitions. The absorption spectrum of the crystal Nd:YAG in the range 4000Å to 10000Å is given in Figure 3 and the related energy levels of a Nd^{3+} ion in a typical crystal lattice are given in Figure 4 [Ref. 5]. At room temperature, the 7500Å(C) and 8000Å(B) excitation bands are the most efficient producers of 1.064μm radiation, but at temperatures above 400°K the 5900Å(F) excitation band becomes dominant [Ref. 6].

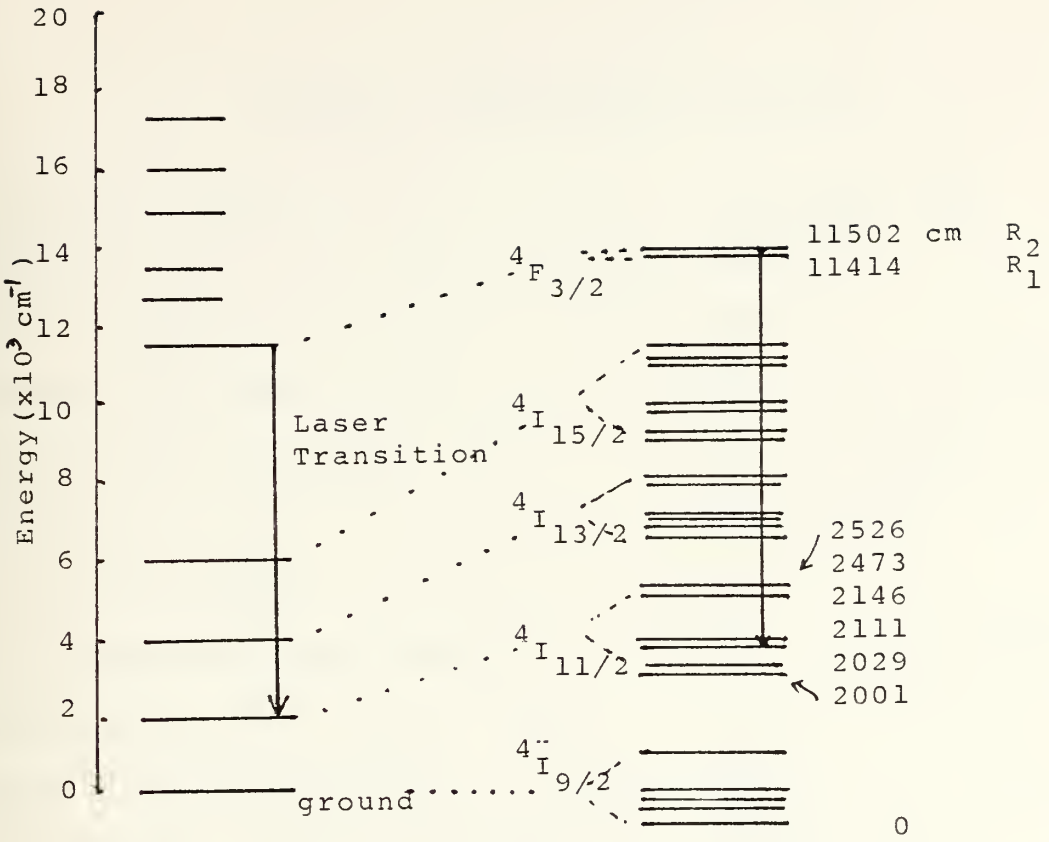

Fig.1 Energy Level Diagram of Nd:YAG

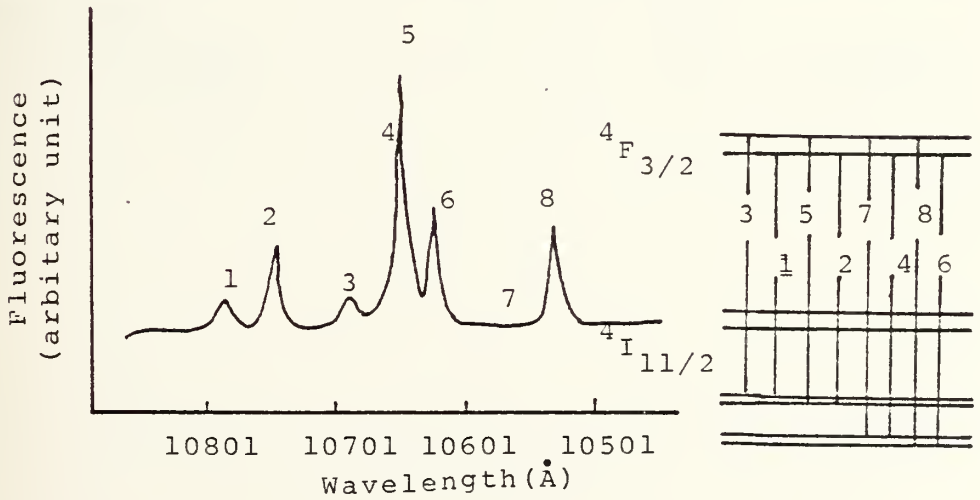

Fig.2 Fluorescence Spectrum of Nd:YAG at 300 °K in the Region of 1.06 μm.

TABLE 1. PROPERTIES OF Nd:YAG

Chemical Formula	$Y_2Al_3O_{12}$: Nd
Melting point	1970°C
Knoop hardness	1215
Thermal expansion	$7.7 - 8.2 \times 10^{-6} °C^{-1}$
Modulus of elasticity	3×10 Kg/cm^2
Density	4.56 g/cm^3
Brewster's angle	61.2°
Stimulated em. cross section	$2.7 - 8.8 \times 10^{-19}$ cm^2
Relaxation time ($^4I_{11/2} \rightarrow {}^4I_{9/2}$)	30 ns
Radiative lifetime ($^4F_{3/2} \rightarrow {}^4I_{11/2}$)	550μs
Spontaneous fluorescence time	230μs
Photon energy at 1.06μm	$h\nu = 1.86 \times 10^{-19}$ J
Thermal conductivity (@ 40°C)	0.029 cal/(sec.°C cm)
Poisson ratio	0.3
Tensile strength	25 - 30 lb/in^2

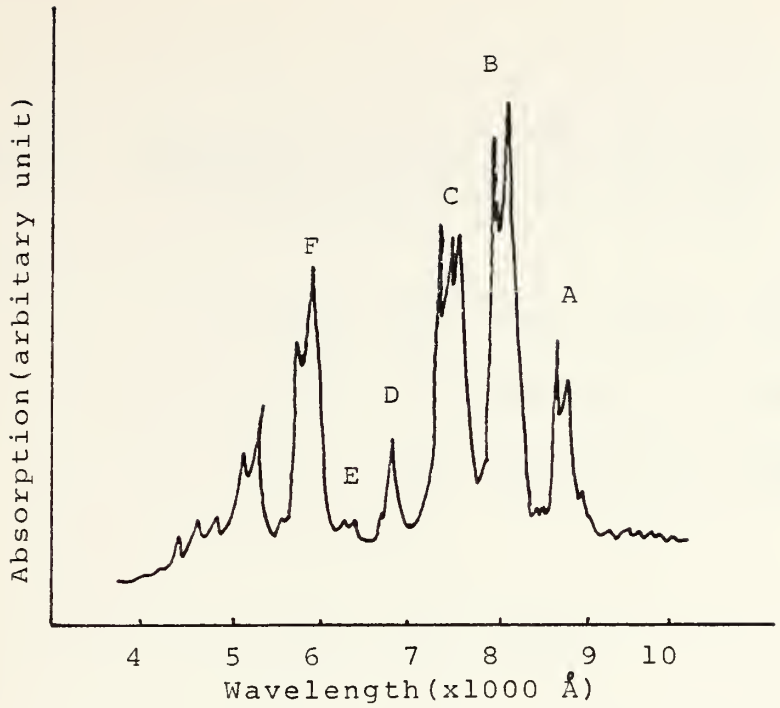

Fig.3 Absorption Spectrum of Nd:YAG

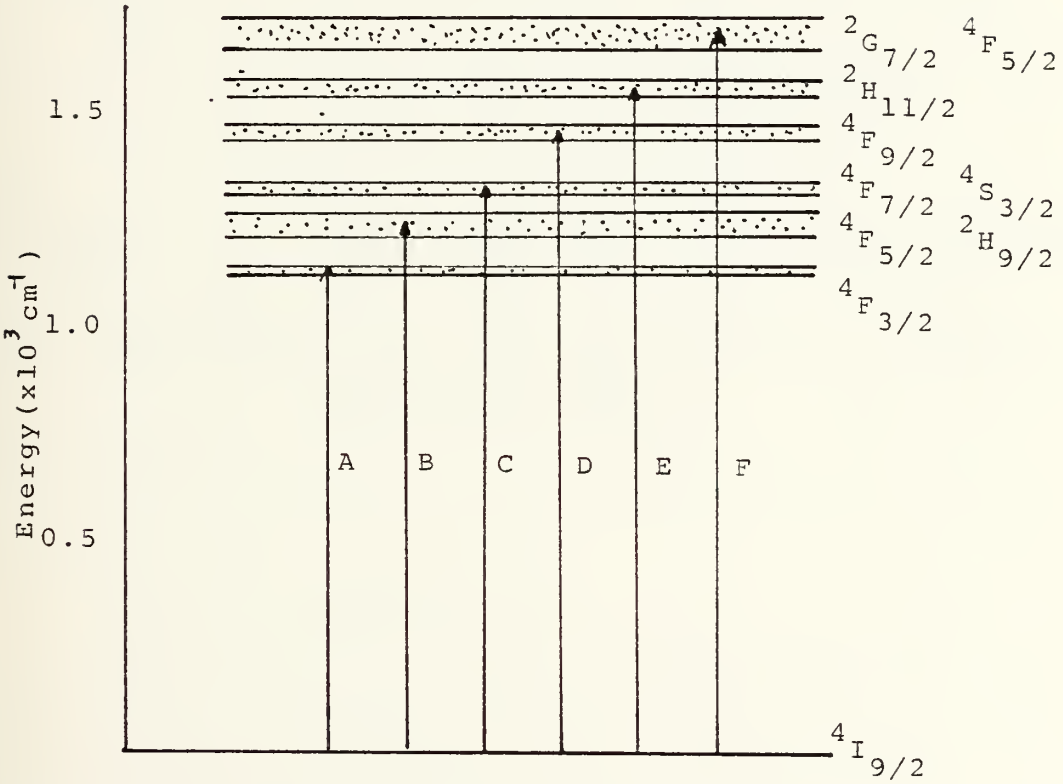

Fig.4 Energy level of Nd:YAG related to Absorption Spectrum

TABLE 2. ABSORPTION SPECTRUM OF Nd IN YAG [REf. 6]

Absorptions (cm^{-1}) at 4.2°K

Assigment							
$^4I_{1/2}$	2010	2037	2111	2146	2473	2526	
$^4I_{13/2}$	3875	3985	4010	4032	4490	4560	
$^4I_{15/2}$	5770	5820	5948	5978	6585	6645	6755
$^4F_{3/2}$	11419	11519					
$^4F_{5/2}$	12369	12427	12517				
$^4H_{9/2}$	12572	12605	12621	12820	12873		
$^4F_{11/2}+^4S_{3/2}$	1337	12435	13563	13570	13594	13633	
$^4F_{9/2}$	14638	14689	14797	14826	14919		
$^2H_{11/2}$	15745	15833	15952	16091	16105		
$^2G_{11/2}+^4G_{5/2}$	16852	16989	17044	17241	17263	17322	17570
$^4K_{13/2}+^4G_{11/2}+^2G_{9/2}$	18784	18823	18839	18985	19470	19569	
$^2K_{15/2}$	20718	20761	20783				

B. OPTICAL RESONATOR

Optical resonators are used primarily in order to build up large field intensities with moderate input. A universal measure of this property is the "quality factor", Q, of the resonator. Q is defined by the relation

$$Q = \omega \frac{\text{field energy stored by resonator}}{\text{power dissipated by resonator}}$$

The light emitted by most lasers contains several discrete optical frequencies, separated from each other by frequency differences which can be associated with different modes of the optical resonator. It is common practice to distinguish two types of resonator modes: "Longitudinal" modes differ from one another only in their oscillation frequency; "Transverse" mode differs from one another in their field distribution in a plane perpendicular to the direction of propagation in addition to differing in their oscillation frequency. The spectral characteristics of a laser, such as linewidth and coherence length, are primarily determined by the longitudinal modes, and the beam divergence, beam diameter and energy distribution are governed by the transverse modes.

1. Resonator Configuration

The most commonly used laser resonators are constructed with two coaxial mirrors for which the spot radii at the mirrors are; [Ref. 7]

$$\omega_1^4 = \left(\frac{\lambda R_1}{\pi}\right)^2 \frac{R_2 - L}{R_1 - L} \frac{L}{R_1 + R_2 - L}$$

$$\omega_2^4 = \left(\frac{\lambda R_2}{\pi}\right)^2 \frac{R_1 - L}{R_2 - L} \frac{L}{R_1 + R_2 - L}$$

where R_1 and R_2 are the radii of curvature of the two mirrors, L is the separation distance between the two mirrors, ω_1 and ω_2 are radii of the spots at the mirrors, ω_0 is the radius of the waist of the Gaussian beam profile, and t_1 and t_2 are the distances of the beam waist (ω_0) from the mirrors.

The radius of the beam waist, which can be formed either inside or outside the resonator, is given by

$$\omega_0^4 = (\lambda/\pi)^2 \frac{L(R_1 - L)(R_2 - L)(R_1 + R_2 - L)}{(R_1 + R_2 - 2L)}$$

The distances t_1 and t_2 between the waist and mirrors are

$$t_1 = \frac{L(R_2 - L)}{R_1 + R_2 - 2L}$$

and

$$t_2 = \frac{L(R_1 - L)}{R_1 + R_2 - 2L}$$

These equations treat the most general case of the stable resonator. There are many different types of resonators that may possibly be constructed. The most widely

used resonator geometries in Nd:YAG laser systems are confocal and plane-concave.

a. Mirrors of Equal Curvature

With $R_1 = R_2 = R$, the radii of the spots at the morrors are

$$\omega_{1.2}^2 = \left(\frac{\lambda R}{\pi}\right) \frac{L}{2R - L}$$

The beam waist, which occurs at the center of the resonator, gives, $t_1 = t_2 = R/2$

$$\omega_0^2 = \left(\frac{\lambda}{2\pi}\right) [L(2R - L)]^{\frac{1}{2}}$$

If we assume that the mirror radii are large compared to the resonator length, $R >> L$ then

$$\omega_{1.2}^2 = \omega_0^2 = \left(\frac{\lambda}{\pi}\right) \left(\frac{RL}{2}\right)^{\frac{1}{2}}$$

A special case of the symmetrical configuration is the spherical resonator which consists of two mirrors separated by twice their radius, $R = L/2$. The corresponding beam consists of modes whose dimensions are fairly large at each mirror and which focus down to a diffraction-limited point at the center of the resonator.

Another special case, where $R = L$, the symmetrical confocal, gives

$$\omega_{1.2} = \left(\frac{\lambda R}{\pi}\right)^{\frac{1}{2}} \quad \text{and} \quad \omega_0 = \frac{\omega_{1.2}}{\sqrt{2}}$$

The confocal resonator (where $R = L$) gives the smallest possible beam waist for a resonator of given length.

b. Plane-Concave Resonator

For a resonator with one flat mirror ($R = \infty$) and one concave mirror,

$$\omega_1^2 = \omega_0^2 = \left(\frac{\lambda}{\pi}\right)[L(R_2 - L)]^{\frac{1}{2}}$$

and

$$\omega_2^2 = \left(\frac{\lambda}{\pi}\right) R_2 \frac{L}{R_2 - L}$$

The beam waist ω_0 occurs at the flat mirror. A special case of this resonator is the hemiconfocal resonator. The hemiconfocal resonator consists of one spherical mirror and one flat mirror placed approximately at the focal point of the sphere. The resulting mode has a relatively large diameter at the spherical mirror and focuses to a diffraction limited point at the plane mirror.

2. Stability of Laser Resonator

The ability of an optical resonator to support low diffraction loss modes depends on the mirror separation L and the radii of curvature, R_1 and R_2. Light rays that bounce back and forth between the spherical mirrors of a laser resonator experience a periodic focusing action. The effect on the rays is the same as in a periodic sequence of lenses. Rays passing through a stable sequence of lenses are periodically refocused. For an unstable system the rays

become more and more dispersed the further they pass through the sequence. In an optical resonator operated in the stable region, the wave propagates between reflectors without spreading appreciably. This fact can be expressed by the stability criterion;

$$0 \leq (1 - \frac{L}{R_1})(1 - \frac{L}{R_2}) \leq 1$$

3. Losses in Optical Resonator

The common loss mechanisms in optical resonators are divided into three groups.

a. Reflection Loss

Loss resulting from imperfect reflection; reflection loss is unavoidable, since without some transmission no power output is possible. In addition, no mirror is ideal: absorption and scattering reduce the reflectivity to somewhat less than 100 percent.

b. Absorption and Scattering Loss

Absorption and scattering in the laser medium; transitions from some of the atomic levels, which are populated in the process of pumping to higher levels, constitute a loss mechanism in optical resonators when they are used as laser oscillators. Scattering from inhomogeneities and imperfections is especially serious in a Nd:YAG crystal.

c. Diffraction Loss

Diffraction loss; the energy propagating beam modes extend to considerable distance from the axis. When a resonator is formed by 'trapping' a propagating beam between two reflectors, it is clear that for finite dimension reflectors some of the beam energy will not be intercepted by the mirror, and will therefore be lost. Figure 5 [Ref. 8] shows the diffraction loss of a number of low-order confocal resonator modes. A is the mirror radius and L is the mirror spacing. The pairs of numbers under the arrows refer to the transverse-modes l,m .

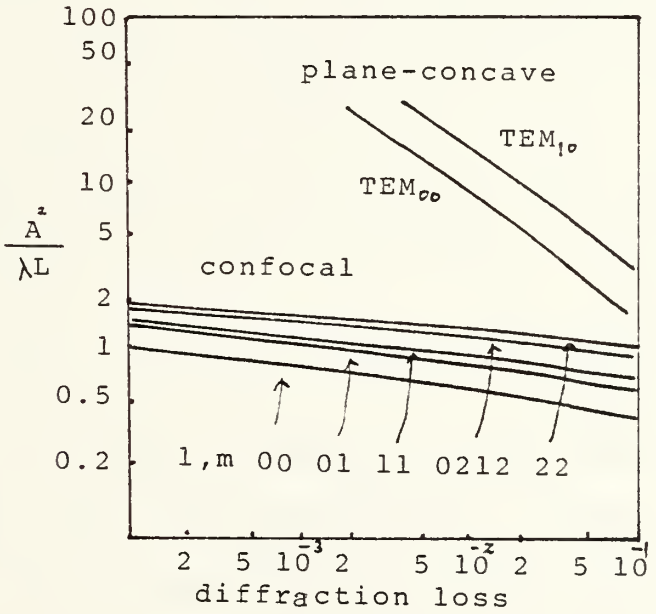

Fig.5 Diffraction losses for resonators.[Ref.8].

C. OPTICAL PUMPING SYSTEM

In optical pumping the light from the light source is concentrated in the laser active material. The atoms are pumped into the upper energy level by absorbing the energy emitted from an incoherent lamp. It is required that the output spectrum bands of the power source should be matched with absorption bands in Nd:YAG, and the pumping cavity should transfer the energy to the active material efficiently. Krypton, xenon and tungsten lamps are widely used as pumping sources. To increase the efficiency, well-designed pumping cavities are required for better concentration and uniform pumping density on the active material.

1. Pumping Sources

A tungsten filament lamp can operate as a black-body emitter at a color temperature of about 3400°K with peak output around 0.85 micrometers. It is a very convenient pumping source for Nd:YAG, but the input power for such a lamp is limited to 500 W/cm, a limit fixed by the melting point of the tungsten. From a knowledge of the pumping bands of Nd:YAG as shown in Figure 3 and the black-body output from a tungsten iodide lamp it can be estimated that only three-four percent of the electrical input power to the lamp is converted into radiation which is usefully absorbed by Nd:YAG. The tungsten-halide lamps

operate at higher temperature (3200°K) than typical filament lamps. This corresponds to an emission maximum occurring at 8400Å for a black-body radiator. Actually the tungsten filament has an emissivity of 0.35 at 3200°K [Ref. 9].

A water-cooled xenon lamp is a good source of line radiation in the near infrared and it can operate at high input power, up to 2.5 kW/cm. However, the emission lines from the xenon lamp do not match the Nd:YAG absorption lines well. Figure 6 represents the spectral emission of a xenon flash tube operated at high current density [Ref. 10].

A water-cooled krypton arc lamp with strong emission lines in the infrared matches the pump bands of Nd:YAG very well, particularly around 8100Å . It has been found that the useful light output of krypton arc lamps for pumping Nd:YAG lasers increased with bore size, fill pressure and input power [Ref. 11]. The emission spectrum of a typical CW-pumped krypton arc lamp is shown in Figure 7 [Ref. 12].

Figure 8 represents the relative efficiency of three different types of lamp for pumping Nd:YAG [Ref. 13].

Mercury arc lamps, alkali arc lamps, semiconductor diodes, and noble gas lamps have also been treated as pumping sources, but the efficiencies of these are relatively higher than the sources previously described.

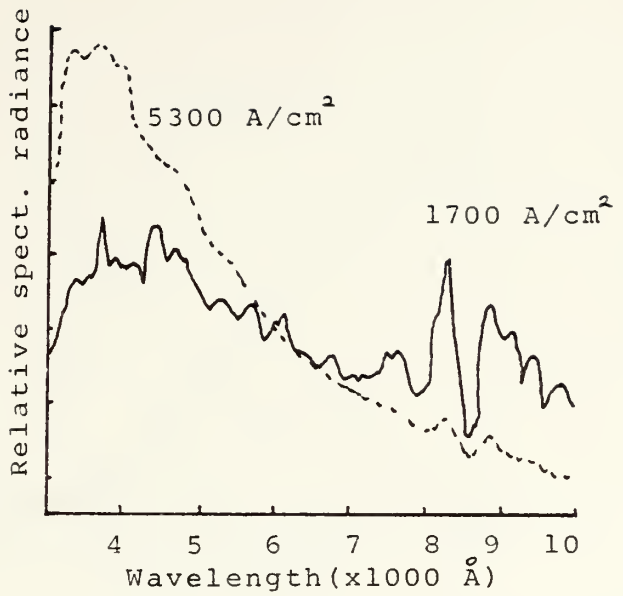

Fig.6 Spectral Emission of a Xenon Flash Tube.[Ref.10].

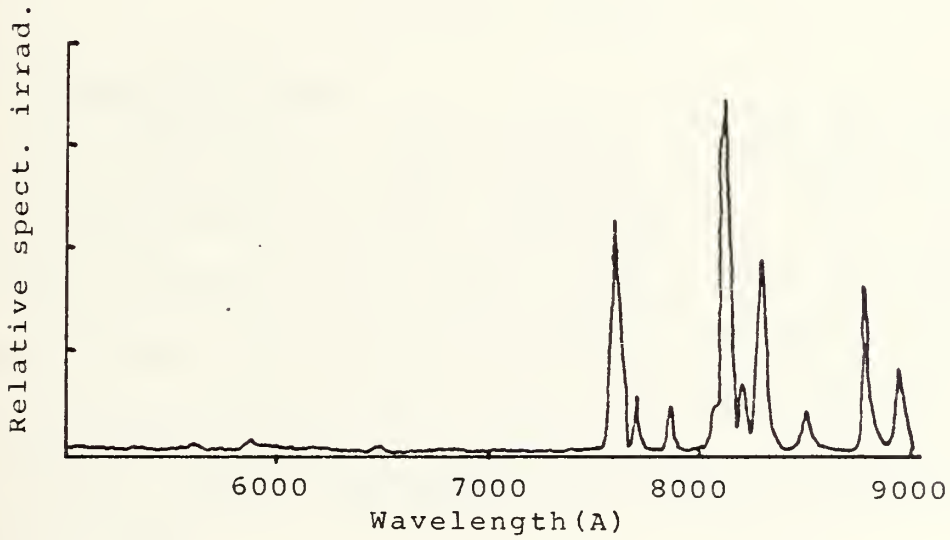

Fig.7 Emission Spectrum of CW-pumped Krypton Aac Lamp(6mm bore, 50mm arc length, 1.3 kW input). [Ref.12].

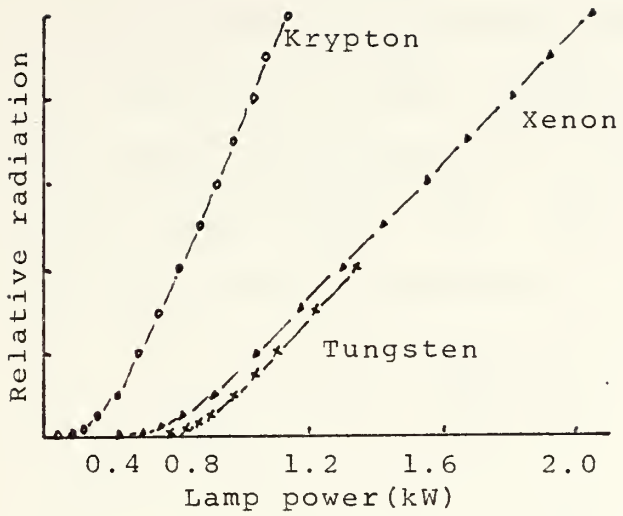

Fig.8 Relative Performance of Krypton,Xenon and Tungsten-iodine lamps for continuous pumping of Nd:YAG. [Ref.13].

2. Pumping Cavities

The efficiency in the transfer of radiation from the source to the active material determines to a large extent the overall efficiency of a laser system. The pump cavity, besides providing good coupling between the source and the absorbing active material, is also responsible for the pump density, and the divergence and optical distortion of the output beam.

The most widely used pumping cavity is a highly reflective elliptical cylinder with the laser rod and

lamp at the focal lines. The elliptic configuration is based on the geometrical theorem that rays originating from one focus of the ellipse are reflected into the other focus. Therefore an elliptical cylinder transfers energy from a linear source placed at one focus to a linear absorber placed along the second focal line. The geometrical cavity transfer coefficient can be expressed by [Ref. 14];

$$n_{ge} = \frac{1}{\pi} [\alpha_0 + (\frac{r_R}{r_L})(\theta_0 - \theta_1)]$$

where

$$\alpha_0 = \cos^{-1}[\frac{1}{e} \{1 - \frac{1 - e^2}{2} (1 + \frac{r_R}{r_L})\}]$$

$$\theta_0 = \sin^{-1}\{(\frac{r_L}{r_R})\sin\alpha_0\}$$

$$\theta_1 = \sin^{-1} (\frac{r_L}{r_R})$$

r_L and r_R are the radii of the lamp source and the rod, and $e = c/a$ where $2c$ is the focal separation and $2a$ is the length of the major axis.

Semi-ellipse, double-ellipse and multi-elliptical cavities can be used for special requirements, and some configurations are shown in Figure 9.

Close-coupled nonfocusing pump cavities, circular or oval in cross section, are also used. However the efficiency of a close-coupled cavity is relatively low. A higher

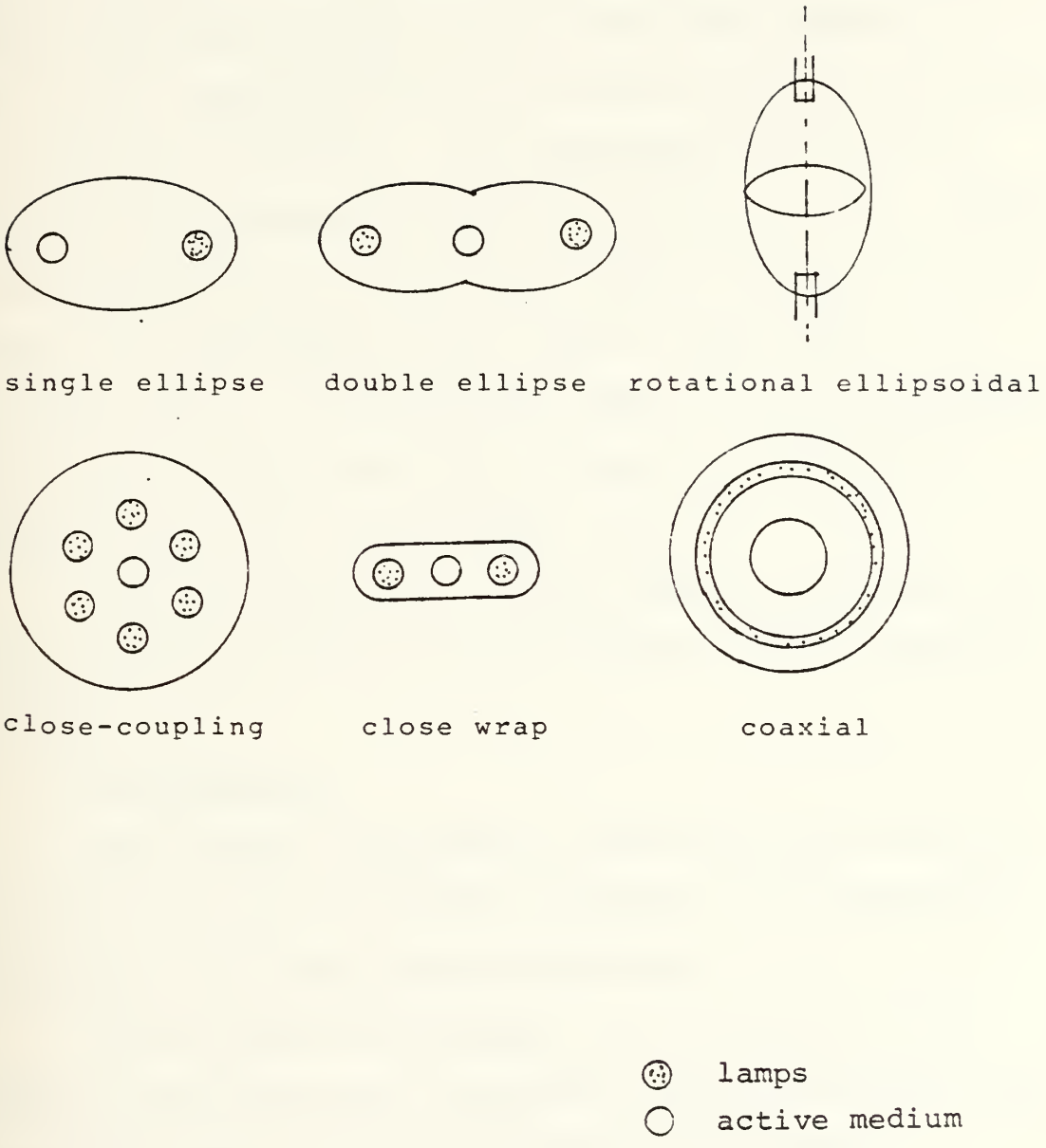

Figure 9. Characteristic Configurations of Pumping Cavity.

energy-transfer efficiency is achieved in pumping systems with reflectors in the form of an ellipsoid of revolution or a sphere. Figure 9 represents various types of cavities.

The material employed in the design of a pump cavity is an important element in the efficiency of the cavity, since the reflectivity of the metal surface as well as the transmission of the cooling fluid in the cavity is wavelength dependent. The reflectivities of cavity surfaces are increased by special treatment, as for example by plating with high reflectance material such as gold or silver. For CW-pumped Nd:YAG lasers, where most of the pumping occurs in the wavelength range 0.7-0.9 micrometers, gold is used almost exclusively because, in contrast to silver, it does not tarnish [Ref. 15].

In this experiment a silver coated quartz tube and a gold coated cylindrical brass tube were used as pumping cavities.

3. Efficiencies

The overall efficiency of the cavity can be split up into three parts; transfer efficiency, lamp radiative efficiency, and pump quantum efficiency.

The transfer efficiency η_t is defined as the ratio of the pump power (or energy) actually entering the rod to the power (or energy) emitted by the lamp.

The lamp radiative efficiency n_i gives the efficiency of conversion of electrical input to light output in the wavelength range λ_1 to λ_2 in which the effective absorption bands of the laser medium lie (e.g., 0.3 to 0.9 micrometers for Nd:YAG). The lamp radiative efficiency is therefore given by:

$$\eta_i = \frac{2\pi RL \int_{\lambda_1}^{\lambda_2} I_\lambda d_\lambda}{P}$$

where R is the radius and L is the length of the lamp, I_λ is the electrical power delivered to the lamp.

The pump quantum efficiency η_a accounts for the fact that not all of the atoms raised to the pump bands subsequently decay to the upper laser level. The quantum efficiency is a quantity over which one can have little control since it depends on the properties of the Nd:YAG crystal.

D. HEAT REMOVAL

Thermal effects in the laser rod are brought about by a combination of heat generation due to absorption of pump radiation and heat flow due to cooling processes. Heating and cooling of the laser material lead to a nonuniform temperature of the rod, which results in a distortion of the laser beam due to a temperature and stress dependent variation of the index of refraction. In addition, optical

distortions can arise as a result of an elongation and bending of the rod.

The cooling methods can be divided into three groups: liquid flow cooling, air or gas cooling and conduction cooling.

1. Thermal Effects in the Laser Rod

The thermal stress in a cylindrical rod, caused by a temperature distribution $T(r)$, can be calculated from the equation of axial stress; [Ref. 16]

$$\sigma_r(r) = QS(r^2 - r_0^2)$$

$$\sigma_r(r) = QS(3r^2 - r_0^2)$$

$$\sigma_z(z) = 2QS(2z^2 - z_0^2)$$

where $S = \alpha E(16K(1 - \nu))^{-1}$ contains the materials parameters; E is Young's modulus; ν is Poisson's ratio; K is the thermal conductivity; and α is the thermal coefficient of expansion. The stress components, σ_r, σ_0, σ_z represent the components of stress in a cylindrical coordinate system. After adding the two stress components $\sigma_z(z)$, $\sigma_r(r)$ vectorially, to obtain

$$\sigma_{max} = \frac{\sqrt{2}\alpha E P_a}{8\pi K(1 - 2)L}$$

then $P_\alpha a$ can be expressed, where $\sigma_{max}=\sigma_t$, as

$$P_a = \frac{8\pi K(1 - \nu)L\sigma_t}{\sqrt{2\alpha E}}$$

Here P_a is the total heat dissipated by the rod and L is the length of the rod. The solution of this equation with the physical properties given in Table 1, indicates that α_{max} is achieved with 115W dissipated as heat per centimeter length of the Nd:YAG rod. The tension on the surface of the rod equals the tensile strength (σ_t) of the material. The actual rupture stress of a laser rod is very much a function of the finish of the rod.

The refractive index changes due to strain are presented [Ref. 17];

$$\Delta n_r = -\frac{1}{2} n_0^3 \frac{\alpha Q}{K} C_r r^2$$

$$\Delta n_0 = -\frac{1}{2} n_0^3 \frac{\alpha Q}{K} C_\phi r^2$$

$$\Delta n_r - \Delta n_0 = n_0^3 \frac{\alpha Q}{K} C_b r^2$$

where C_r , C_ϕ and C_b are functions of the elastooptical coefficients of Nd:YAG; $C_r = 0.017$, $C_\phi = -0.0025$ and $C_b = -0.0097$. Q has dimensions watts/cm and r is measured in centimeters.

The thermal lensing due to refractive index variation can be separated into a temperature- and stress-dependent variation, and one due to end-face curvature. The

change of refractive index due to thermal strain is dependent on the polarization of light: the focal length due to this effect can be represented [Ref. 18] as

$$f' = \frac{K}{QL}\left(\frac{1}{2}\frac{dn}{dT} + \alpha C_{r\phi} n_0^3\right)^{-1}$$

The focal length of the rod caused by an end-face curvature, due to small perturbations on the principal thermal distortion pattern which occurs in the rod near the ends, can be represented as

$$f'' = K[\alpha Q r_0 (n_0 - 1)]^{-1}$$

The combined effect of temperature- and stress-dependent variation of refractive index and the distortion of end-face curvature of the rod leads to the following expression for the focal length;

$$f = \frac{KA}{P_a}\left[\frac{1}{2}\frac{dn}{dT} + \alpha C_{r\phi} n_0^3 \frac{\alpha r_0 (n_0 - 1)}{L}\right]^{-1}$$

where A is the cross-sectional area of the rod.

The thermal stress requires that the rod must be cooled and shielded sufficiently to keep the heat power in the rod below 115 w/cm and to keep $f > R/2$.

2. Cooling Techniques

There are three different cooling techniques available: liquid cooling, air or gas cooling, and conduction cooling. Water, water mixed with alcohol, and

water mixed with ethylene are commonly used coolants for liquid cooling systems. The heat carried out by the coolant can be expressed; $Q = \Delta T.\ C\ .\ m$ where C is the specific heat of the coolant, m is the mass flow rate and ΔT is the temperature difference between inlet and outlet coolant. The choice of coolant is dependent on the operating temperature, corrosion reaction with cavity material, etc. For examples: water cannot be used in military systems which may be operated various temperatures, since malfunction of systems may occur by freezing of the coolant; and fluorinated hydrocarbon coolant cannot be used with 365 aluminum or similar alloys, since hydrofluoric acid formed by UV radiation will react with cavity materials.

A commonly used liquid cooling system consists of a liquid pump, a heat exchanger and a reservoir. Sometimes it contains a demineralizer, deionizer and some sensors for monitoring the coolant flow rate.

An air or gas cooling system can be employed in a low power laser for cooling the laser rod and flash lamp by forced air flow. The air flow required for cooling the laser is calculated at standard conditions (20°C, 1 atm) by;

$$f_{\nu}(\text{liter/min}) = \frac{49P}{\Delta T}\ (\text{W/°C})$$

where ΔT is the temperature difference between inlet air and outlet air.

A conductive cooling effect is achieved by mounting the laser rod either clamped, soldered, or bonded to the heat sink. If the laser rod is clamped to a heat sink, a temperature gradient will develop across the rod-clamp interface. The heat flow is then $Q = \Delta T\ h\ A$ where h is a heat transfer coefficient, A is area of contact between rod and sink, and ΔT is the temperature difference.

In this work, water and air cooling methods were applied using a KWC-3 Laser Cooler manufactured by Union Carbide Company and an electric fan to force air through the cavity.

III. EXPERIMENTAL INVESTIGATION

A. CONSTRUCTION OF THE SYSTEM

The laser system was constructed with three major subsystems: optical resonator, optical pumping system, and cooling system.

1. Optical Resonator

The resonators were built with two mirrors; one flat mirror and the other concave. The properties of the four mirrors which were used in this work are presented in Table 3.

TABLE 3

PROPERTIES OF MIRRORS FOR EXPERIMENTAL LASER SYSTEMS

number	type	transmittance at 1.06μm (%)	focal length(cm)	mirror diameter(cm)
M 1	plane	27 (20)	∞	2.0
M 2	concave	3.5 (0)	42.5	2.0
M 3	plane	6.1 (5)	∞	2.1
M 4	concave	3.0 (0)	77	2.1

* ( ) represents the values given by manufacturer.

Two mirrors (M 1 , M 2) were designed for the KY-2 system manufactured by the Union Carbide Company which has a double elliptical cavity. The other two mirrors were manufactured by Valpey Corporation. Transmittance was measured with a Spectrophotometer manufactured by

Perkin Elmer Incorporation, and the focal length was measured by a beam tracking method with a small Ne-Ne laser.

2. Optical Pumping System

Circular cylindrical reflectors were used as pump cavities with three lamps located inside the cavity at equal distances from the cavity axis.

a. Pumping Cavities

The elliptical pumping cavity configuration has high transfer efficiency, as discussed in chapter II, and initially a double elliptical cavity was designed for this experiment. However, after exploring the available facilities for fabrication it was decided that the design could not be fabricated locally on the time scale of the experiment, and other designs were prepared with cylindrical geometry.

Two circular cylindrical cavities coated with highly reflective materials were used; a silver coated quartz tube with dimensions: 8.0cm length, 5.0cm outside diameter and 1.5mm thickness; and a gold coated brass tube with the same dimensions as the quartz tube except that the wall thickness was 2mm.

Rapid burn-off of silver occurred while measuring the fluorescence power with the silver coated quartz tube, so the gold coated brass tube was used in all later work. Additionally, the brass tube has higher thermal conductivity

than the quartz tube so the cooling efficiency can be increased with it.

b. Pumping Sources

Tungsten-halogen lamps manufactured by General Electric Company were used in this experiment. A Q1000 3/4cl lamp has dimensions 11.8cm total length, 6.0cm filament length, and 0.2cm filament diameter. The filament, which is centered in the bulb by four spiral-shaped supporters, is connected to the external contacts by means of a molybdenum foil ribbon thin enough to deform on expansion rather than fracture the bulb.

This lamp dissipates 1000 watts at 120 volts input voltage, and the typical operating temperature is 3200°K, corresponding to a black-body radiation peak at 0.9μm.

c. Power Supplies

Lamp power was supplied by autotransformers (variacs) which were manufactured by General Radio Company. One autotransformer was connected to each lamp. The pumping power could be adjusted by changing the input voltage to the variacs. Each autotransformer was supplied from an AC wall outlet rated at 20 A maximum current.

3. Cooling System

A KWC-3 Laser Cooler manufactured by Union Carbide Company was used as the main cooling system. This was

designed for the KY-2 system operated at 2000 watts input power. With this laser cooler it was impossible to cool adequately the experimental system pumped by three lamps. A fan was added to cool the inside of the cavity by blowing out the heated air. Lamp envelope deformation occurred when the system operated without the fan and with 3000 watts input and 2.6 G/min coolant flow rate. The temperature difference between input coolant and output coolant was 10°C and the total operating time to failure was less than 30 minutes. With addition of the fan the coolant temperature difference (ΔT) was reduced to 3.2°C and no further lamp envelope deformation occurred.

4. Assembly of the System

The two mirrors and the pumping-cavity head were mounted on an I-beam shaped optical bench, and the power supplies, laser cooler, and an electric fan were connected to the pumping-cavity head. Figure 10 shows the basic assembly of the system.

The pumping-cavity head was build in the Naval Postgraduate School Physics Department machine shop from aluminum and brass. The details of the pumping-cavity head are presented in Appendix A. The head consists of a cylindrical pumping cavity, a laser rod and rod-holder, a cooland flow tube, an outer rectangular body and two end-plates, a base plate, lamp holders, and three lamps.

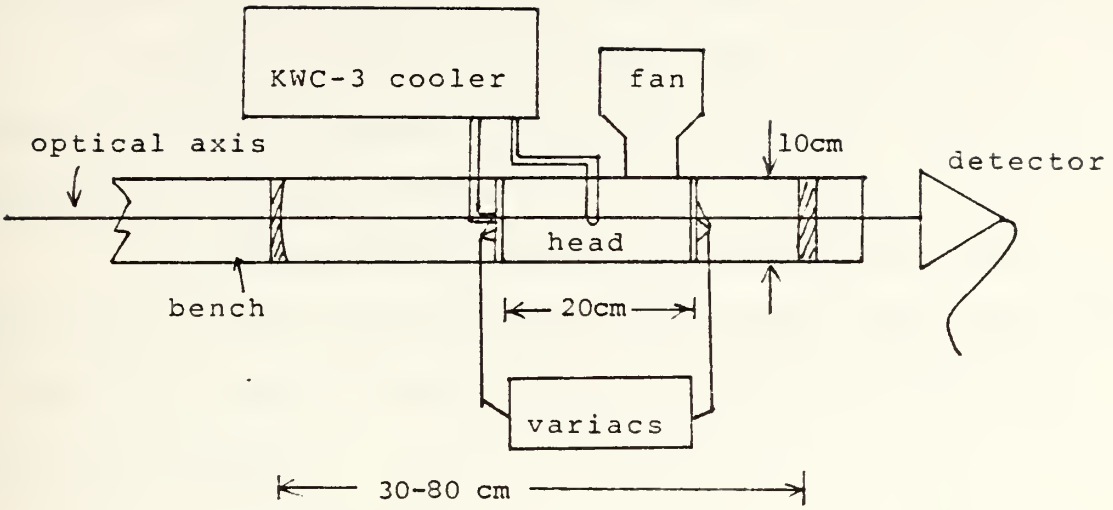

Fig.10 Basic Assembly of Experimental System.

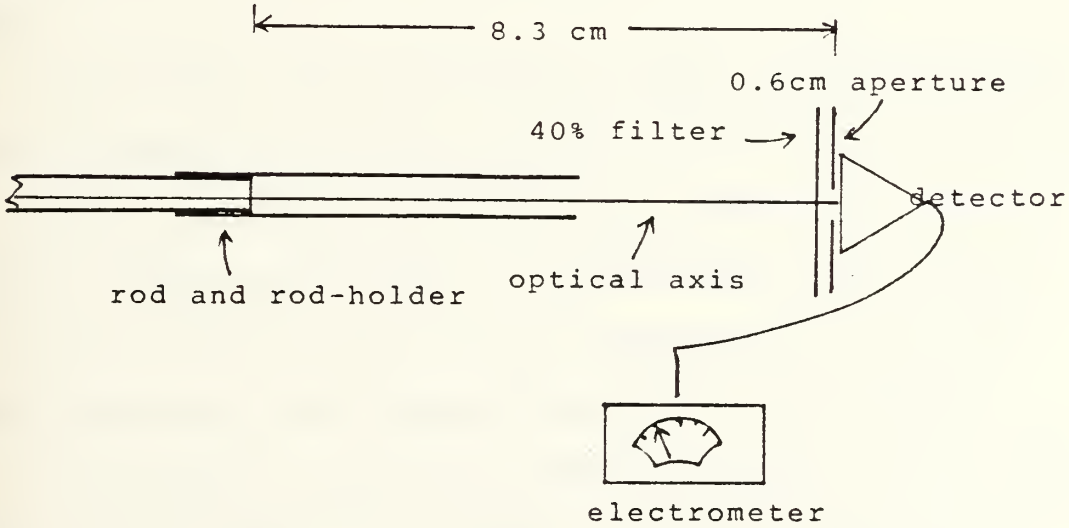

Fig.11 Detector System Alignment

The pumping cavity is located inside the body and these two components are fixed in position with two end plates with two rubber O-rings for sealing. The rod and rod-holder were placed inside the coolant flow-tube which was supported by two holders.

The coolant flows through the coolant flow tube to cool the rod, and flows between the body and the cavity wall to cool the cavity. The air flow is directed through the three lamp holes.

B. OPERATION OF THE LASER

1. Measurement of Fluorescence

The emitted fluorescence radiation power emitted from the rod is the commonly used measure of the level of population inversion, and hence gain, in a laser active medium.

To monitor the fluorescence power, a PIN-10DP photo-diode manufactured by United Detector Technology Incorporation was used with an optical filter whose trasmittance was 40 percent at wavelength 1.06μm. The PIN-10DP diode has the properties; $1cm^2$ of active area, responsivity 0.35 W/A at 1.06μm wavelength, and $10mW/cm^2$ maximum light intensity.

Fluorescence power was measured on the optical axis within a solid angle of $1.3x10^{\pi}Sr$, with a 0.6mm aperture at a distance 8.3cm from the endface of the rod. The optical

filter was mounted directly in front of the detector. Figure 11 shows the detector system alignment.

First, the fluorescence power of the KY-2 laser system was measured to determine the threshold fluorescence power, since the rod of the experimental laser system has the same dimensions as the rod of the KY-2 system. The measured fluorescence power is plotted in Figure 12. The KY-2 system began lasing at 90V input, corresponding to 2.0×10^{-3} W/dA of fluorescence power, where dA is the area of detector aperture. With the assumption that the experimental laser has an identical rod to the KY-2 system, the measured fluorescence power at 90 volts of input power was estimated as a threshold fluorescent power for the experimental system. The measured fluorescent power of the experimental laser is also plotted in Figure 12. The maximum detectable power of the PIN-10DP diode within the 0.6mm diameter of the aperture was calculated as 2.8×10^{-3}W.

2. Measurement of Laser Output

The laser output was measured for two different selections of the resonator mirror sets. The resonator was tuned using a He-Ne laser, by adjusting the mirror mounts to align the beams reflected from the two rod end faces and from the resonator mirrors. Table 4 represents the measured maximum output and the possible resonator mirror sets.

These measurements were made using the gold coated brass cavity reflector.

TABLE 4

LASER ACTION WITH DIFFERENT COMBINATIONS OF MIRRORS

reflecting mirror	output mirror	output power at 3300W input(watts)
M 2	M 1	0
M 4	M 1	0
M 2	M 3	1.65
M 4	M 3	2.05

Lasing action was not observed with M 1 as output mirror, due to its high transmittance, which raised the threshold power above that attainable with the system as constructed. With 6.1 percent output mirror and a spacing of 35cm, a maximum of 2.05 watts output was detected. The measured output is presented in Figure 13 as a function of input power. 3300 W is the maximum input power of the experimental system with 130 V input voltage.

Threshold input power was 2200 W which agrees with estimated input power from the measurement of fluorescence power as discussed previously. The overall efficiency of the experiemtal system was calculated as 0.06 percent, and the maximum slope efficiency, achieved at 3300 watts input power, was 0.19 percent.

1.65 watts maximum output was detected with M 2 and M 3 as a set of resonator mirrors.

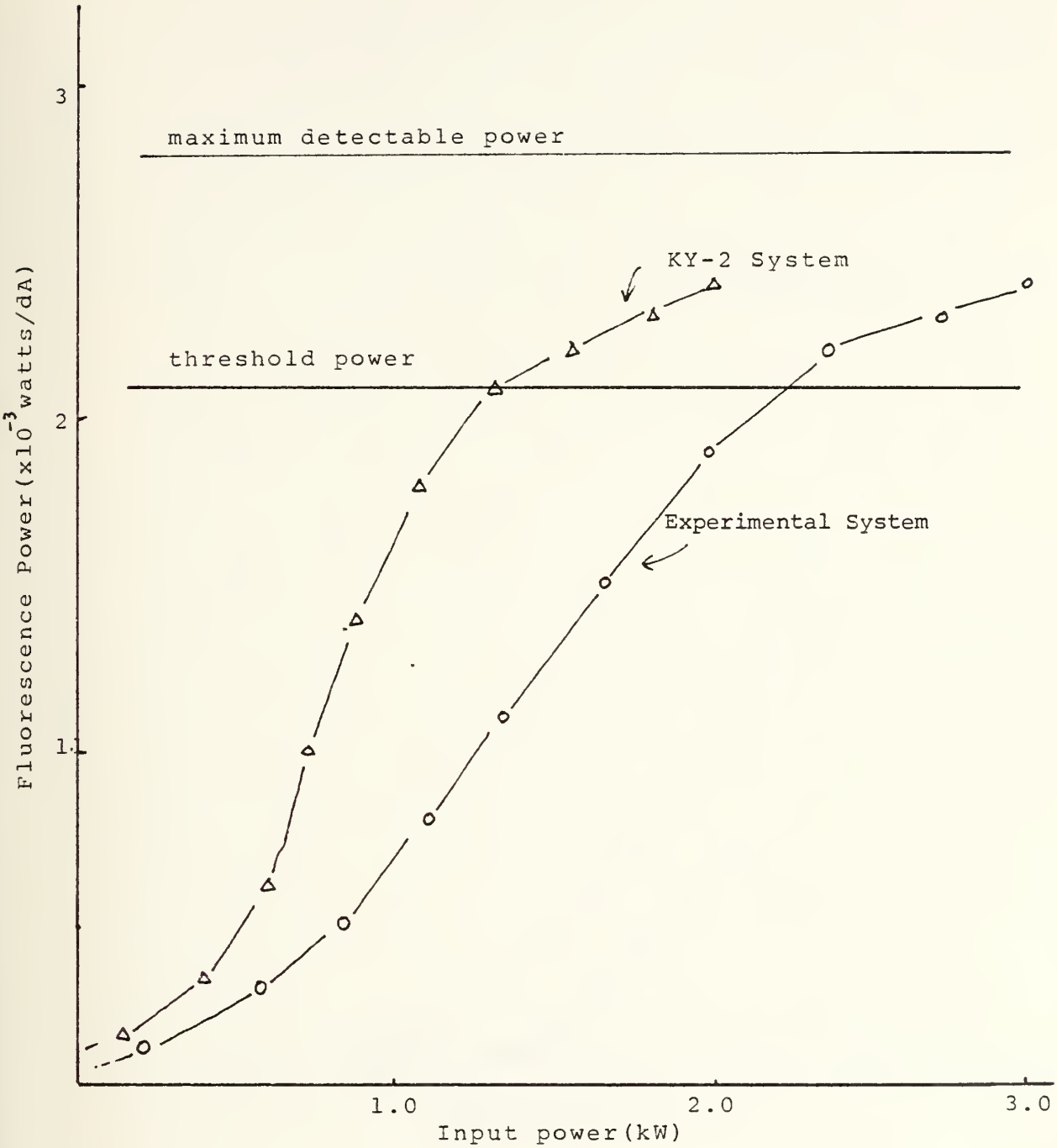

Fig.12 Measurement of Fluorescence power

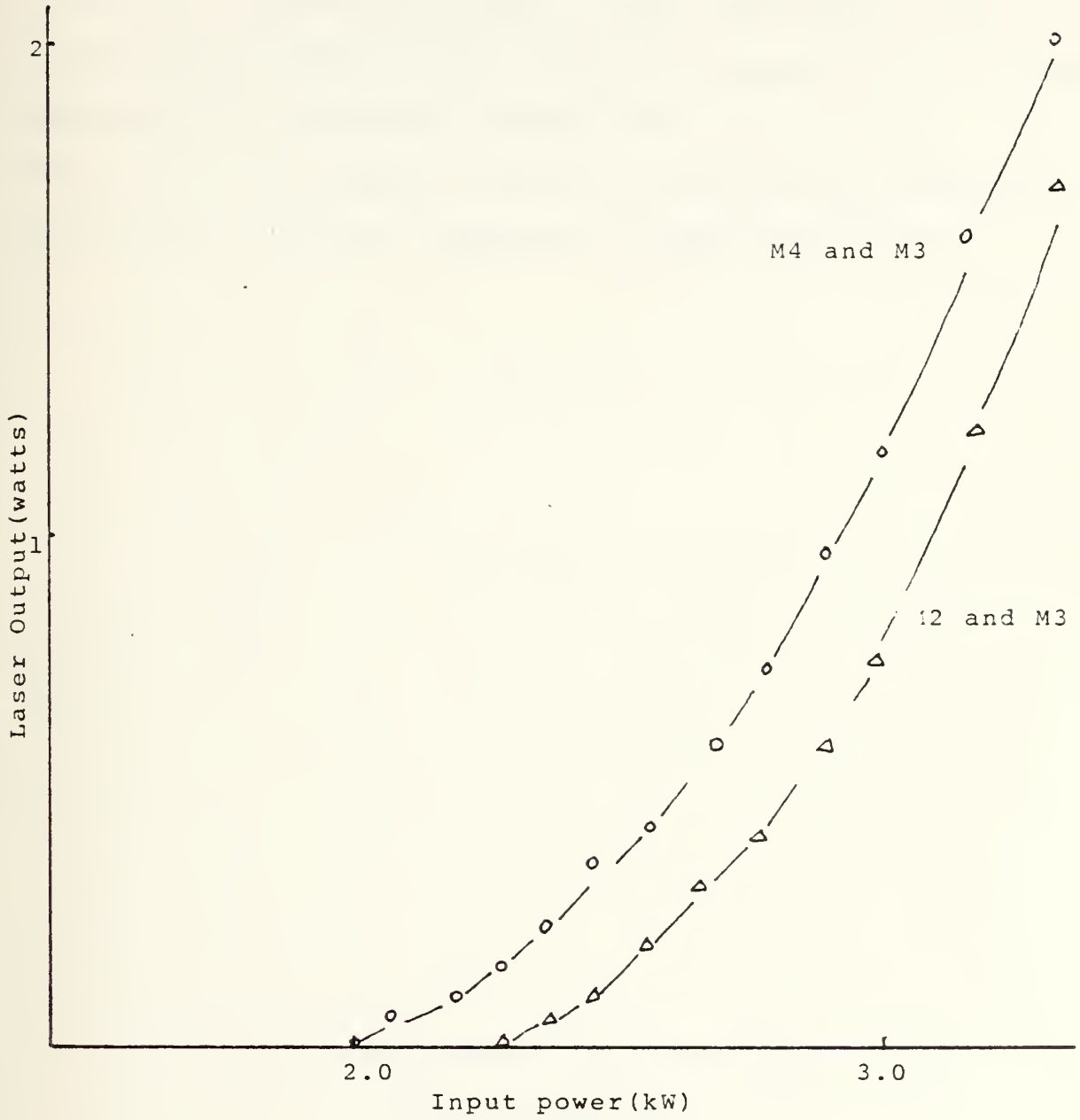

Fig.13 Laser Output of the Experimental System.

The maximum output was measured with varied spacing of the resonator mirrors with the results shown in Figure 14. The maximum output of the experimental laser system with the gold coated cavity was measured with different spacings of the resonator mirrors from 0.3m to 0.85m, where 0.3m is the minimum possible spacing of the resonator due to the size of the components between the mirrors.

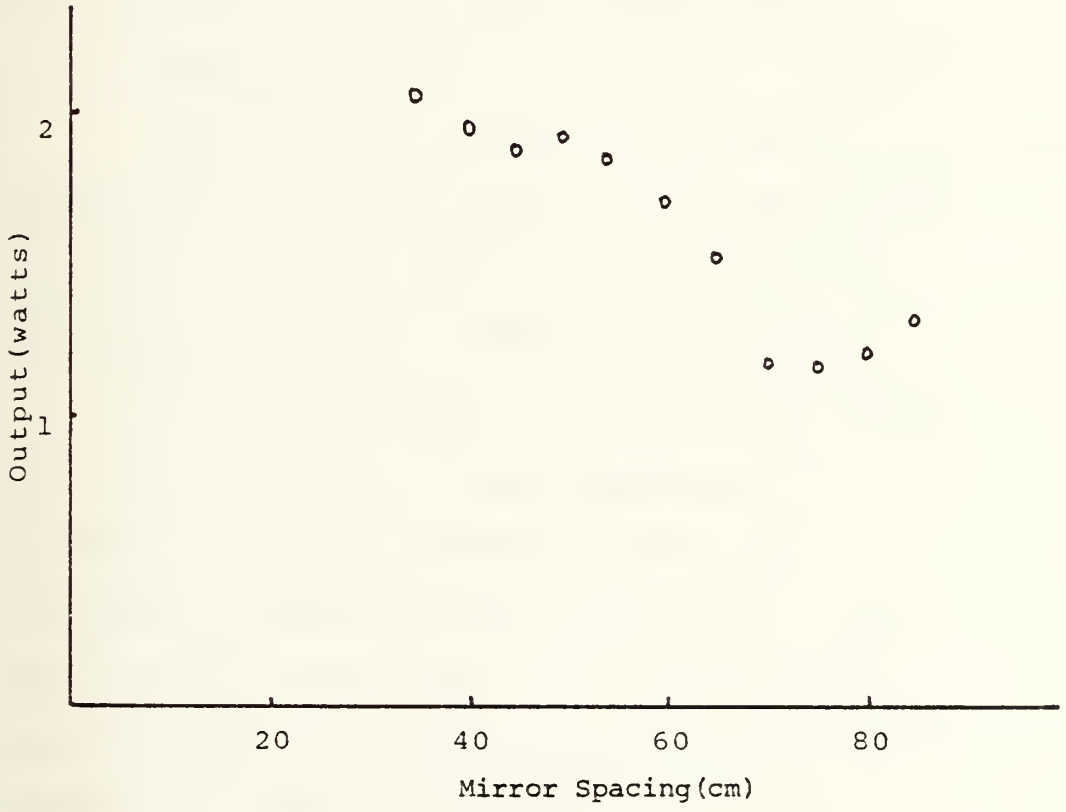

Fig.14 Maximum Output with Change of the Spacing of the Resonator Mirror.

C. DISCUSSION

The transmittance of the output mirrors strongly affects the laser action as described in Table 3. With M 3 as the output mirror laser output was detected, but with M 1 it was not detected.

The maximum output of the experimental laser system increased as the spacing of the two mirrors decreased as shown in Figure 14.

The relation between input power and output power does not satisfy the linear relationship expected.

1. Resonators

The selection of the transmittance of the output mirror is an important factor in the laser system. In the case of the four level laser, the following condition should be satisfied for laser action, [Ref. 19];

$$(1 - T_i)^2(1 - T_1)(1 - T_2)(1 - a)^2 EXP(2\sigma N_c L) = 1$$

where T_1 and T_2 are the transmittances of the two mirrors, a is the fractional mirror loss, T_i is the fractional internal loss per pass, σ is the cross-section for the laser transition, N_c is the critical population inversion for laser action, and L is the length of the Nd:YAG rod. With the assumption that T_i , a , and T_2 are small enough to neglect, the equation can be written as;

$$(1 - T_1)EXP(2N_c\sigma L) = 1$$

which gives

$$N_c = -\ln(1 - T_1)/2\sigma L$$

With $L = 6.3\text{cm}$, $\sigma = 3.5 \times 10\text{cm}$, $T_{1.M3} = 0.061$ and $T_{1.M1} = 0.27$, the calculated values of N_c are;

$$N_{c.M3} = 1.4 \times 10^{16} \text{ atoms/cm}^3$$

$$N_{c.M1} = 7.1 \times 10^{16} \text{ atoms/cm}^3$$

Even considering the effects of T_i, a, and T_2 the ratio of $N_{c.M1}$ to $N_{c.M3}$ is;

$$\frac{N_{c.M1}}{N_{c.M3}} \doteq \frac{\ln(1 - T_1)}{\ln(1 - T_3)} \doteq 5$$

If we assume the linear increase of fluorescence power with increasing input power (Figure 10) to extend to threshold with M 2, the threshold should be at approximately five times that for M 1, i.e., about 10mW/dA.

The maximum output power of the experimental system decreased with increasing separation of the two mirrors. The output power of a CW laser depends on the volume of active medium occupied by the oscillating mode (or modes), and can be represented as [Ref. 20];

$$P = A_e I_s \frac{\gamma_1}{2} \left(\frac{P_{in}}{P_{th}} - 1\right)$$

Here A_e is the equivalent cross-sectional area of laser medium occupied by the oscillating mode (or modes), I_s

is the saturation intensity expressed as $I_s = h\nu/\sigma I$, where τ is the spontaneous fluorescence time (230μs), and γ_1 is the logarithmic loss of output mirror ($\gamma_1 = -\ln(1 - T_1)$).

To recognize the reasons for the increase of maximum output with decrease in the resonator spacing, it is necessary to solve the relation between the resonator spacing and A_e . The area A_e can be expressed as, $A_e = \pi\omega_0^2\ 1/4$, at the beam waist for the TEM_{00} mode. But in the general case many modes are in oscillation in the resonator, so that the solution for A_e becomes complicated. A suitable solution has not been obtained at this time.

2. Measurements of Fluorescence and Output Power

The PIN-10DP detector has low maximum detectable intensity as shown in Figure 12, and may be saturated at higher power levels in Figure 12. Thus it is necessary to replace the photo detector to provide better reliability of measurement of fluorescence at high input power.

The measured laser output does not show the expected linearity with input power, since the pumping efficiency changes due to mismatch between the emission spectrum of the lamps and absorption spectrum of the Nd:YAG. The emission spectrum of the tungsten-halide filament lamp has a black-body radiation distribution, while the absorption spectrum of the Nd:YAG is sharply selective, as shown in Figure 3. The peak radiation wavelength decreased as input

power decreased; thus the slope efficiency decreased with decreasing input power. The maximum slope efficiency occurs at the point where the peak radiation wavelength of the tungsten lamp coincides with the main absorption bands of the Nd:YAG.

The highest observed value of output power, 2.05 watts, was achieved with 130 volts input voltage to the three lamps. The maximum recommended input voltage of the tungsten filament lamps is, however, limited to 120 volts for 3200°K filament temperature and long lifetime of lamps.

3. Efficiency

The cylindrical cavity has low transfer efficiency compared to the elliptical cavity. In a modified close-coupled cavity, the transfer efficiency is dominated by the radiation directly intercepted by the rod without reflection from the cavity wall. For this reason the lamps should be placed as close as possible to the rod for maximum transfer efficiency of the cavity. The minimum spacing between the filament and rod centers in the cavity is 1.0cm, at which the lamp envelopes and the coolant flow tube are in contact. To avoid lamp fractures caused by inadequate cooling, it is necessary to separate the rod and the lamp envelopes. In this work the separation of lamp from rod was 1.2cm.

The krypton arc lamp should have better pumping efficiency and larger input power per unit length, as seen in chapter II.

It is recommended that the cylindrical close-coupled cavity be replaced by an elliptical cavity and/or the pumping sources changed from tungsten filament lamps to Kr arc lamps for improvement of the efficiency.

4. Cooling

The maximum cooling ability of the KWC-3 cooler was found to be 1.6kW without increase of reservoir temperature, with 3.0°C temperature differenc between inlet and outlet coolant and 2.0 G/min coolant flow rate. At the flow rate of 2.0G/min, 4.5°C of temperature rise was required for removal of 80 percent of a 3000 watts input.

Without the electric fan the temperature of the reservoir increased continuously, and finally lamp envelope deformation occurred. With the additional air cooling fan, 35 percent of the emission power could be removed by the fan and 65 percent of the emission power could be removed by the KWC-3 cooler without increase in inlet temperature at 3000 watts input power. The measured temperature difference was 3.2°C at a coolant flow rate of 2.5G/min.

IV. CONCLUSION

Laser action has been detected in an experimental laser system constructed with a circular cylindrical cavity and pumped by three tungsten-halide filament lamps. The efficiency of the system was very low, due to the low transfer efficiency of the cavity.

To improve the slope efficiency, several factors should be considered; 1) transfer efficiency of the cavity, 2) radiation efficiency of the lamps, 3) transmittance of the output mirror, and 4) optimization of the spacing of the resonator mirrors to fill the maximum volume of active medium with oscillating modes.

It will also be necessary to improve the cooling system, since there are power losses through the air blow-out holes located on the end-plates.

With 6.1 percent transmittance at the output mirror and 35cm resonator spacing, a maximum of 2.05 watts output was detected at 3300 watts input power. To prolong the lifetime of the lamps it is recommended that the input voltage not exceed 120 volts. With 120 volts input voltage to three lamps, 1.15 watts output power was measured, and the system can be cooled without increase in the temperature

of the reservoir. This means the experimental system can be operated continuously at the lower output.

One interesting experimental result is the decrease in maximum output power with increasing spacing of the resonator mirrors. Two design factors which might account for this change are the increase in spot size on the mirror with increase in spacing, causing additonal diffraction loss, and decrease in the gaussian waist size, leading to a decrease in the resonant mode power overlapping with the laser rod.

It is desirable to solve the relationship between spacing of the resonator mirrors and the effective rod volume occupied by oscillating modes at a given location of the optical axis.

The other promising area to pursue is optimization of the transmittance of the output mirror for maximum output with given pumping conditions.

APPENDIX A

DETAILS OF PUMPING-CAVITY HEAD

The pumping-cavity head was built in the Naval Postgraduate School Physics Department machine shop using brass for the cavity reflector and aluminum for the other parts.

The body assembly consists of a circular cylindrical cavity, two end-plates, a cavity-holder, and two O-rings for sealing. These components were fixed with eight screws.

A body assembly and two holders were put on the bed and fixed by eight screws with three O-rings for sealing. The water inlet and outlet tubes were installed on the bed and cavity assembly.

More details are presented in the following figures.

CONTENTS

figures

A.1 Components of the Pumping-Cavity Head

A.2 Cross Section View of Body Assembly

A.3 Front View of Holder

A.4 Cross Section View of Holder Assembly

A.5 Rod and Rod-Holder

A.6 Bed

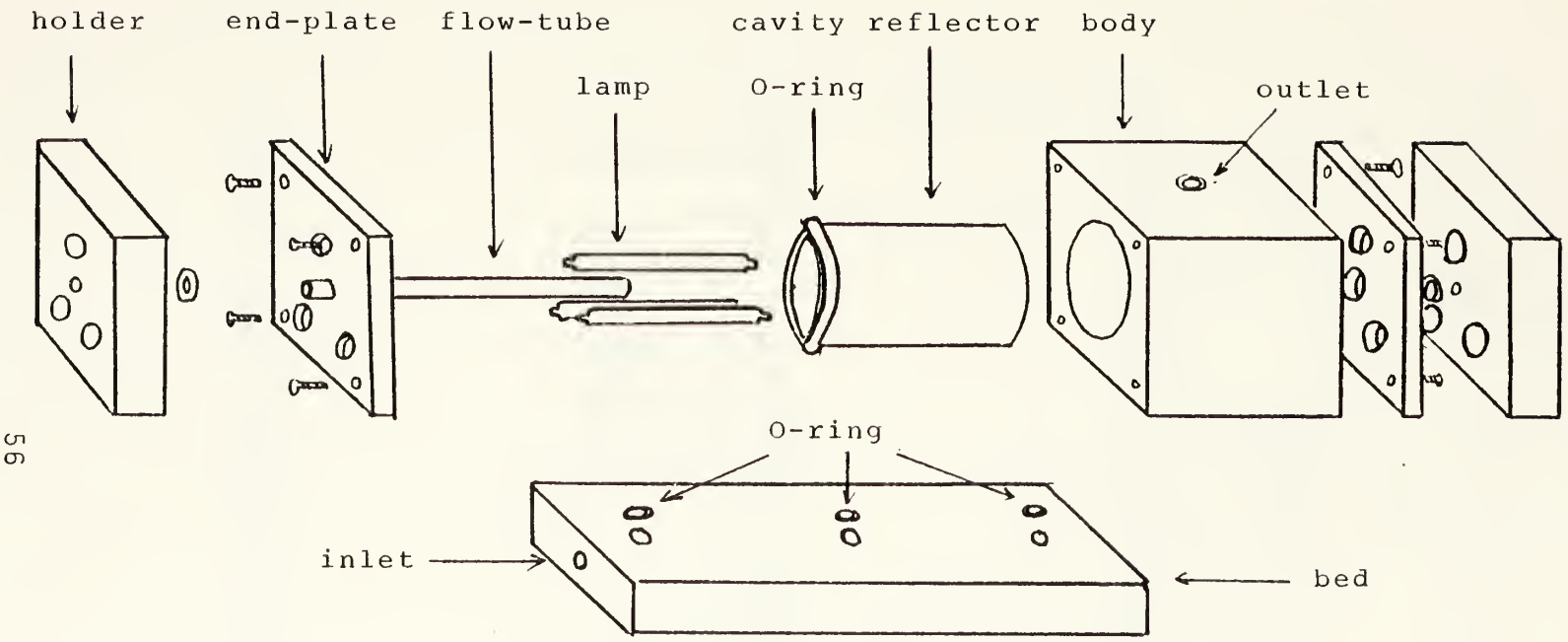

Fig.A1 Components of the Pumping-Cavity-Head

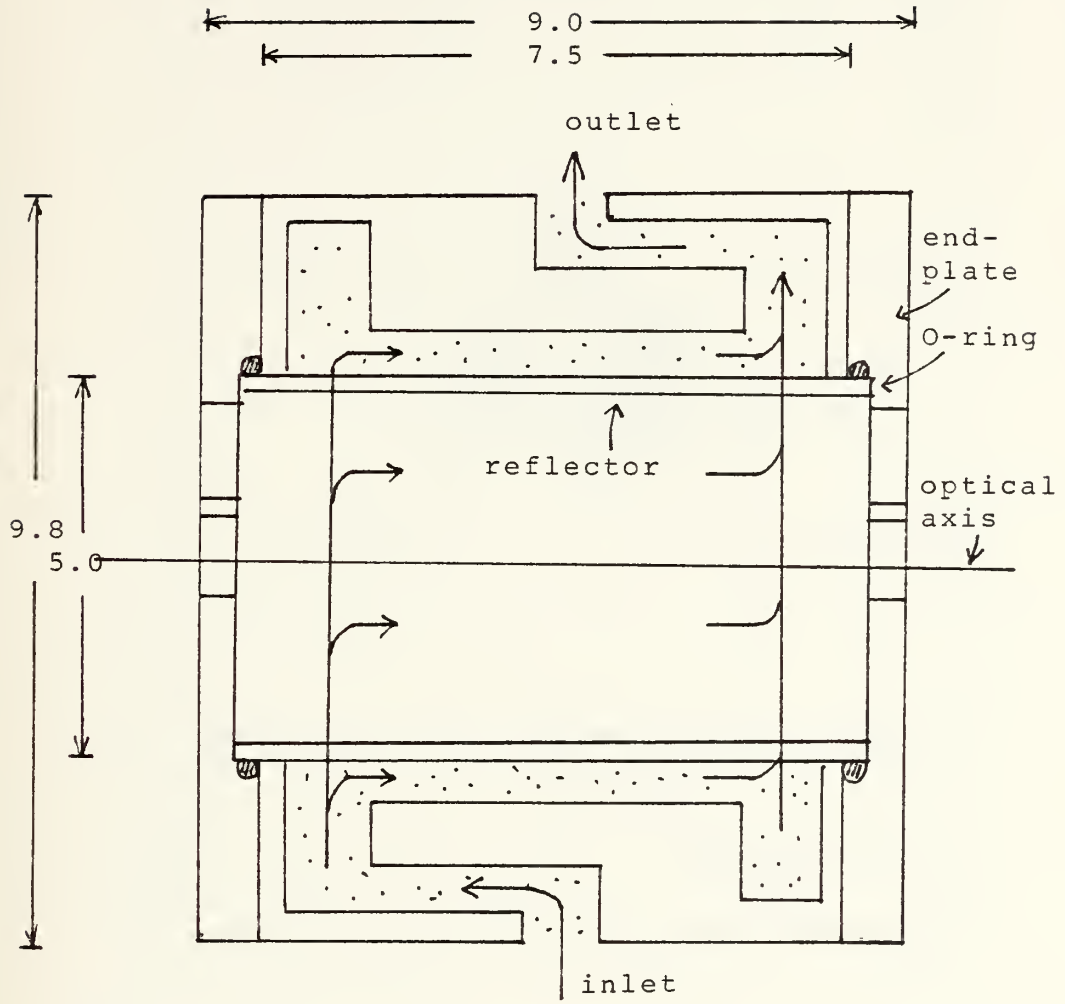

Fig.A2 Cross-Section View of Body Assembly
(→ represents coolant flow)

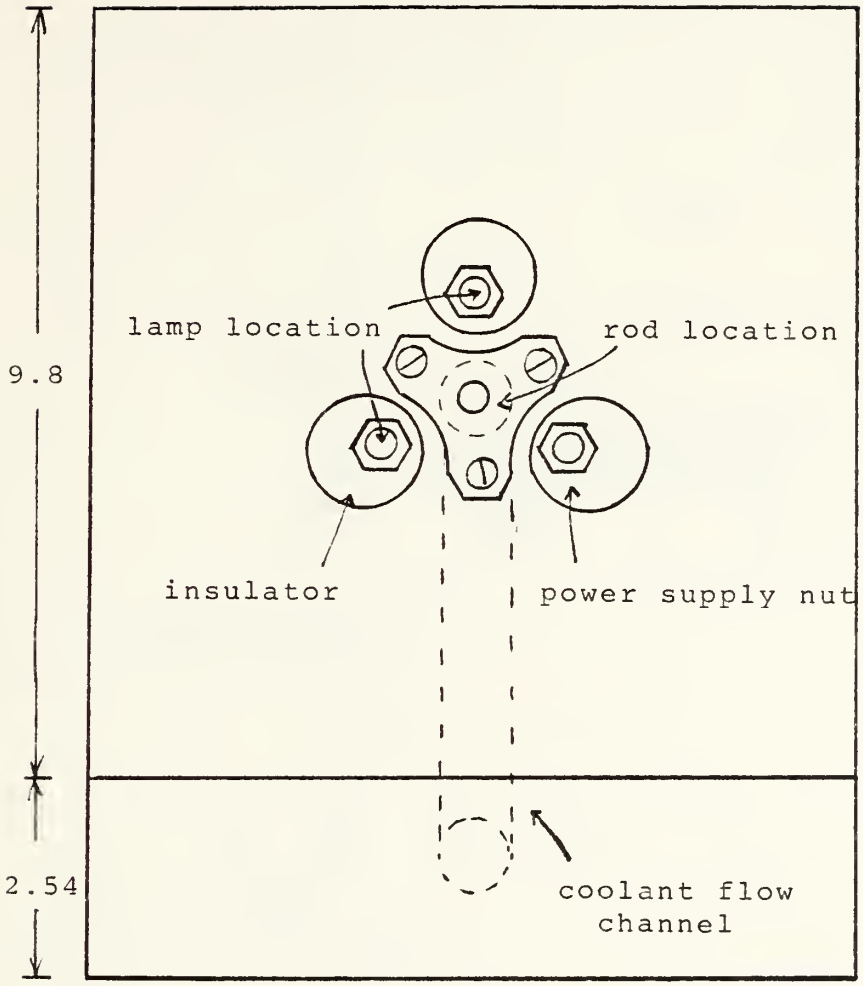

Fig.A3 Front View of Holder

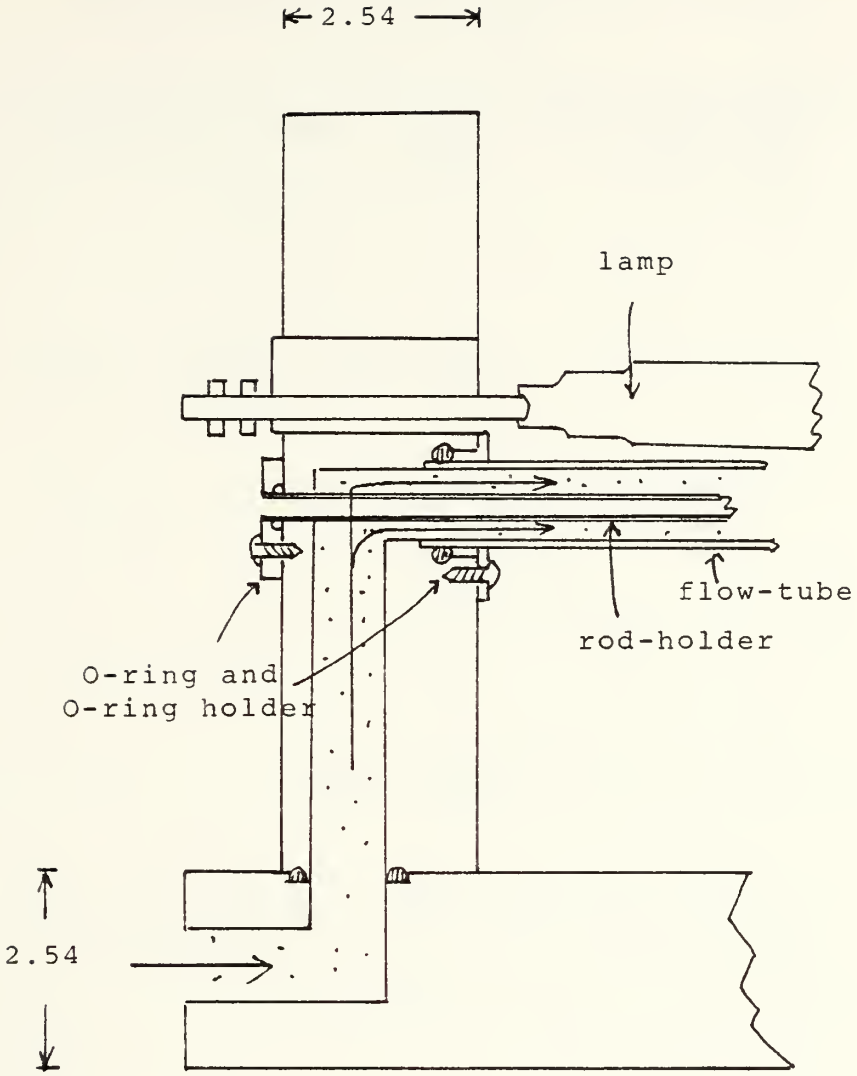

Fig.A4 Cross Section View of Holder Assembly
(→ represents coolant flow)

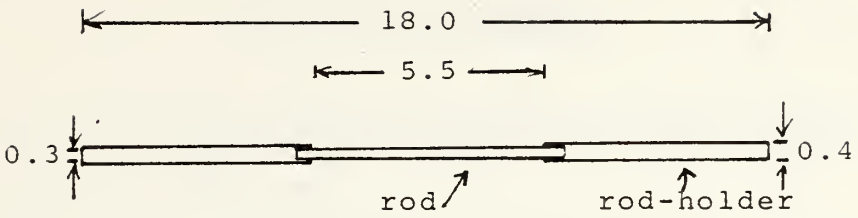

Fig.A5 Rod and Rod-Holder

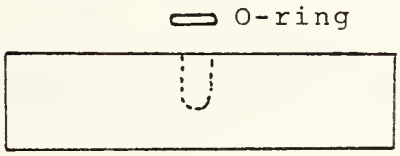

side view

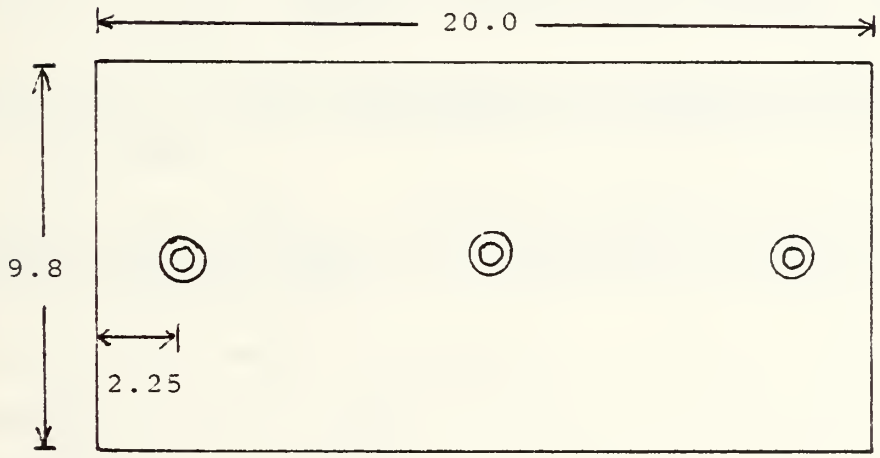

top view

Fig.A6 Bed

LIST OF REFERENCES

1. Jung, J. W., The Construction of a Nd:YAG Laser, Master's Thesis, Naval Postgraduate School, Monterey, California, June 1982.

2. Goodwin, D. W., Advances in Quantum Electronics, p. 92, Academic Press Inc., 1979.

3. Koechner, W., Solid State Laser Engineering, p. 55, Springer-Verlag New York, Inc., 1976.

4. Koechner, W., p. 56.

5. Siegman, A. E., An Introduction to Lasers and Masers, p. 20, McGraw Hill Book Co., 1971.

6. Goodwin, D. W., p. 95.

7. Kogelnik, H., Lasers, pp. 295-347, Marcel Dekker, New York, 1966.

8. Boyd, G. D., Gordon, J. P., Confocal Multimode Resonator for Millimeter through Optical Wavelength Masers, Bell System Tech. J., Vol. 40, p. 498, (1961).

9. Cooper, A. W., Sensors, Signals and Systems, NPGS lecture note, p. B7/8, 1983.

10. Goncz, J. H., New Developments in Electric Flashtubes, Instrument Society of America Transactions, Vol. 5, p. 28, 1966.

11. Grasis, M., Reed, L., Longlife Krypton Arc Lamp for Pumping Nd:YAG Laser, ILC Technology, Inc., pp. 9-12 and pp. 30-35, 1973.

12. Grasis, M., Reed, L., p. 78.

13. Goodwin, D. W., p. 78.

14. Koechner, W., p. 309.

15. Koechner, W., p. 327.

16. Timoshenko, S., Goodier, J. N., Theory of Elasticity, McGraw Hill, New York, 1951.

17. Foster, J. D., Osternik, L. M., Thermal Effects in a Nd:YAG Laser, J. Appl. Phys. 41, 3656, 1970.

18. Koechner, W., p. 353.

19. Svelto, O., Principles of Lasers, p. 152, Plenum Press, New York and London, 1982.

20. Svelto, O., p. 154.

INITIAL DISTRIBUTION LIST

		No. Copies
1.	Defense Technical Information Center Cameron Station Alexandria, Virginia 22314	2
2.	Library, Code 0142 Naval Postgraduate School Monterey, California 93943	2
3.	Physics Library, Code 61 Department of Physics and Chemistry Naval Postgraduate School Monterey, California 93943	1
4.	Professor A. W. Cooper, Code 61Cr Department of Physics and Chemistry Naval Postgraduate School Monterey, California 93943	4
5.	Professor J. R. Neighbours, Code 61Nb Department of Physics and Chemistry Naval Postgraduate School Monterey, California 93943	1
6.	Maj. Chung, Ki Hyun, Korea Army 182 Kenae-Ri Pyengseng-up Pyungtak-Kun Kyunggi-Do, 180-11, Republic of Korea	5
7.	Library of K.M.A Kongneng P.O. Box 77 Dobong-Gu, Seoul, Rebublic of Korea	2